Stargazin Interaction With Serine Racemase Mediates Cerebral Ischemia/Reperfusion Injury in Rats

Xiaqing Yuan
First Affiliated Hospital of Soochow University
Shanshan Diao
First Affiliated Hospital of Soochow University
Shujun Chen
First Affiliated Hospital of Soochow University
Jiajie Lu
First Affiliated Hospital of Soochow University
Haitao Shen
First Affiliated Hospital of Soochow University
Haiying Li
First Affiliated Hospital of Soochow University
Xiang Li
First Affiliated Hospital of Soochow University
Jiang Wu
First Affiliated Hospital of Soochow University
Chao Liu
Soochow University
Ya Yang
Soochow University
Qun Xue
First Affiliated Hospital of Soochow University
Qi Fang
First Affiliated Hospital of Soochow University
Hongru Zhao
First Affiliated Hospital of Soochow University
Lei Gan
Second Affiliated Hospital of Soochow University
Jianqiang Ni
First Affiliated Hospital of Soochow University
Haifeng Lu (lu.haifeng110@163.com)

First Affiliated Hospital of Soochow University https://orcid.org/0000-0002-8100-2184
Juehua Zhu
First Affiliated Hospital of Soochow University
Gang Chen
First Affiliated Hospital of Soochow University

Research Article

Keywords: D-serine, stargazin, serine racemase, MCAO/R, NMDAR

Posted Date: October 28th, 2021

DOI: https://doi.org/10.21203/rs.3.rs-999457/v1

Abstract

D-Serine is thought to be involved in N-methyl-D-aspartate (NMDA)-type glutamate receptor-mediated neurotoxicity and plays a pathophysiologic role in stroke. D-Serine is synthesized by serine racemase (SR), which directly converts L-serine into D-serine. The deletion of SR has been reported to protect against cerebral ischemia damage. Additionally, SR catalytic activity is physiologically regulated by its binding to stargazin. However, whether the stargazin-SR interaction affects the level of stroke damage remains elusive. We showed that cerebral ischemia increased the interaction of stargazin and SR and decreased the levels of D-serine. Disrupting the stargazin-SR interaction by knocking down stargazin aggravated cerebral ischemic insults. We found that cerebral ischemia decreased the phosphorylation of stargazin at the Thr-321 residue, which was phosphorylated by cAMP-dependent protein kinase A (PKA). Treatment with the PKA inhibitor H89 blocked stargazin T321 phosphorylation, augmented the stargazin-SR interaction, decreased D-serine levels, and alleviated focal cerebral ischemic damage in rats subjected to middle cerebral artery occlusion and reperfusion (MCAO/R). Thus, the stargazin-SR interaction is a promising strategy in the treatment of stroke.

Introduction

Cerebral ischemia is a major cause of human neurological morbidity and mortality, and is associated with a poor prognosis worldwide. Cerebral ischemia is caused by an interrupted blood supply to the brain and can result in severe neurodegeneration and vascular dementia in patients [1].

Glutamate, the main excitatory neurotransmitter of the mammalian central nervous system (CNS), activates α-amino-3-hydroxy-5-methyl-4-isoxazolepropionic acid (AMPA), N-methyl D-aspartate (NMDA), and kainate (KA) receptors [2]. NMDA receptor (NMDAR) is essentially a receptor-gated calcium ion channel with high permeability to calcium and sodium ions [3]. Immediately following ischemia, glutamate accumulates at synapses, leading to widespread stimulation of NMDARs, causing intracellular calcium overload and neurotoxicity [4-7]. It is recognized that activation of NMDARs requires the binding of both glutamate and glycine. D-serine is a physiologic coagonist with glutamate at NMDARs and is involved in NMDA receptor-induced neurotoxicity [8,9]. Serine racemase (SR) is an enzyme that converts L-serine to D-serine and its deletion has been reported to protect against cerebral ischemia and excitotoxicity [10]. The enzymatic activity of SR is enhanced by binding to PICK1 (protein interacting with C kinase 1) [11,12] and glutamate receptor-interacting protein [13], which are proteins associated with AMPA receptors. In contrast, SR activity is inhibited by binding to the phospholipid phosphatidylinositol 4,5-bisphosphate [14] and S-nitrosylation, which occurs following activation of NMDARs [15].

Stargazin (γ-2) is a member of the family of related transmembrane AMPA receptor regulatory proteins (TARPs), and it was initially recognized for the important role it plays in AMPA receptor trafficking [16]. SR binds to the C-terminal of stargazin, which promotes membrane localization of SR and inhibits SR catalytic activity. AMPA receptor activation leads to the association separation of SR and stargazin in the membrane, leading to enhanced catalytic activity of SR and increased generation of D-serine [17].

We hypothesized that the Stargazin-SR interaction mediated D-serine release in penumbral tissue and may play a critical role in the sustainment of post-ischemic neuronal injury. In this study, we identified an increased interaction between Stargazin-SR in the Sprague-Dawley (SD) rat model of MCAO/R-induced brain injury. We also devised genetic deletion and pharmacology experiments in the penumbral tissue and investigated the role and underlying mechanisms of the Stargazin-SR complex in MCAO/R-induced brain injury.

Materials And Methods

Experimental Animals

All of the procedures were approved by the Ethics Committee of the First Affiliated Hospital of Soochow University and conformed to the Animal Research: Reporting In Vivo Experiments (ARRIVE) guidelines. Male SD rats weighing 250–300 g were purchased from the Experimental Animal Center of the Chinese Academy of Sciences (Shanghai, China). All of the rats were housed at a comfortable temperature (22°C) and relative humidity (50%) under a regular light/dark (12 h/12 h) schedule. Water and food were available ad libitum. Sample numbers were decided by power analysis during the animal ethics dossier application.

Establishment of the Experimental Middle Cerebral Artery

Occlusion/Reperfusion Model in SD Rats

We constructed the experimental middle cerebral artery occlusion/reperfusion (MCAO/R) experimental model as described previously. Briefly, SD rats were anesthetized and fixed under the operating microscope. Then, the right common carotid artery (CCA), the internal carotid artery (ICA), and the external carotid artery (ECA) were carefully exposed through the cervical midline incision. Next, a part of the filament with a rounded tip coated with poly-L-lysine was inserted into the CCA, through the bifurcation, along the right ICA until the entrance of the middle cerebral artery (MCA) was occluded. Body temperature was maintained between 36.5°C and 37.5°C using a heating pad during the procedure. After 2 h of ischemia, the filament was withdrawn to restore the blood flow. The inclusion and exclusion criteria of the MCAO/R rats referred to the Longa score, which was evaluated on a scale from 0 to 4 as follows: 0 = no observable deficits; 1 = failure to fully extend the left forepaw, mild neurological deficits; 2 = circling to the left side when walking, moderate neurological deficits; 3 = falling to the left side when walking, severe neurological deficits; and 4 = no spontaneous walking with a decreased level of consciousness. Rats with a score of 1–3 were included in the study, and those with a score of 0 or 4 were excluded. In the sham group, operations were similar to those in the MCAO/R group, except that no filament was inserted to block the MCA blood flow. The rats were killed at 1, 3, 6, or 24 h after MCAO/R model onset. After 24 h of reperfusion, the brain tissue of rats was obtained separately for 2,3,5-triphenyltetrazolium chloride (TTC) staining. In this model, the penumbra (peri-infarct) region around the ischemic core can be rescued, and the study focused on the role of stargazin in the penumbra region.

Cell Culture

Primary rat cortical neurons were obtained and cultured as described previously. Briefly, cortical neurons were prepared from embryonic-day-18 brains. Then, cortical neurons were digested with 0.25% trypsin-EDTA solution for 5 min at 37°C. The dissociated neurons were seeded on to six-well plates (Corning, Steuben, NY, USA) precoated with poly-D-lysine (Sigma Aldrich, St. Louis, MO, USA), and were cultured in neurobasal medium containing 2% B-27, 0.5-mM GlutaMAX, 50 U/mL of penicillin, and 50 U/mL of streptomycin (all from Invitrogen, Grand Island, NY, USA) under humidified air containing 5% CO_2 at 37°C. The medium was renewed every 2 days until cell confluency was reached.

Antibodies and Drugs

Rabbit anti-Stargazin antibody (D33G3; Cell Signaling Technology, Danvers, MA, USA) was used for western blotting, immunofluorescence analysis, and co-immunoprecipitation. Rabbit anti-Stargazin antibody (ab254037) was used for western blot and was obtained from Abcam (Cambridge, MA, USA). Mouse anti-Serine racemase antibody (612052) was used for co-immunoprecipitation and was obtained from BD Transduction Laboratories (San Diego, CA, USA). Mouse anti-Serine racemase antibody (sc-365217), which was used for immunofluorescence analysis, and protein A/G PlUS-Agarose (sc-2003) were obtained from Santa Cruz Biotechnology (Dallas, TX, USA). Normal rabbit IgG (#2729) and normal mouse IgG (#5873) was obtained from Cell Signaling Technology. Rabbit anti-STG-pT321 antibody was customized by Abclonal (Wuhan, China). Rabbit anti-β-Tubulin antibody (4466) was purchased from Cell Signaling Technology. PKA inhibitor H89 (S1643) was obtained from Beyotime Institute of Biotechnology (Shanghai, China). Secondary antibodies for western blotting, including horseradish-peroxidase-conjugated goat anti-rabbit (sc-2004) and anti-mouse (sc-2005) Abs, were obtained from Santa Cruz Biotechnology. Secondary antibodies for immunofluorescence analysis, including Alexa Fluor-555 donkey-anti-mouse IgG antibody (A31570) and Alexa Fluor-488 donkey anti-rabbit IgG antibody (A21206), were purchased from Invitrogen (Carlsbad, CA, USA).

Western blotting

The brain tissue homogenate collected from SD rats was cytolyzed in RIPA buffer (Beyotime, Shanghai, China). The samples were centrifuged at 12,000 × g for 10 min at 4°C. Then we acquired the supernatant liquid and measured the protein concentration using enhanced BCA Protein Assay Kits (Beyotime). An 80-μg aliquot of protein extract from each group was loaded onto a 10% sodium dodecyl sulphate (SDS) polyacrylamide gel, separated, and electro-transferred onto a nitrocellulose membrane (Millipore Corporation, Billerica, MA, USA). Subsequently, the membrane was blocked in 5% nonfat milk for 1 h at room temperature. Following incubation, we incubated the membrane with the primary antibody overnight at 4°C. Then, after incubation of the corresponding HRP-conjugated anti-rabbit or anti-mouse secondary antibodies for 1 h at room temperature, the bands were revealed through an enhanced chemiluminescence kit (Beyotime Institute of Biotechnology) and the relevant data were generated using

ImageJ 1.49 software (National Institutes of Health, Bethesda, MD, USA). The measurable analysis was carried out by observers who were blind to the experimental groups.

Immunofluorescence Analysis

During the in vivo experiments, the brain tissue samples were fixed in 4% paraformaldehyde, embedded in paraffin, cut into 4-μm sections, and dewaxed immediately before staining. Finally, sections were observed using a fluorescence microscope (OLYMPUS BX50/BX-FLA/DP70; Olympus Co., Tokyo, Japan) or a laser scanning confocal microscope (ZEISS LSM 880, Carl Zeiss AG, Oberkochen, Germany). A minimum of six random sections from each group were assessed, and representative results were displayed. We analyzed the relative fluorescence intensity using ImageJ software, and the quantitative analysis was performed by observers who were blinded to the experimental groups.

Coimmunoprecipitation

Immunoprecipitation was performed as described previously. Briefly, the brains of rats subjected to a sham or MCAO/R procedure were harvested, and the penumbral regions were chilled on ice and briefly washed with ice-cold artificial cerebrospinal fluid. Protein extracts were homogenized in RIPA lysis buffer (P0013; Beyotime, Shanghai, China). Supernatants (500 μg) were then incubated with 2-μg Stargazin antibody or normal rabbit IgG (negative control) for 3 h at 4°C with rotary agitation. The antibody-bound complexes were combined with 20-μL Protein A/G PLUS-Agarose and incubated overnight at 4°C with rotary agitation. Bound proteins were eluted by heating at 100°C in 20 μL 2× loading buffer and analyzed using immunoblotting.

Gas/Liquid Chromatography Analysis

The brain tissue homogenates collected from SD rats were cytolyzed in ultrapure water. The samples were centrifuged at 14,000 × g for 40 min at 4°C. Then, we acquired the supernatant liquid for gas/liquid chromatography analysis. For high-performance liquid chromatography (HPLC), a 2.1 mm*100 mm, 1.9-μm C18 chromatographic column (Hypersil Gold; Thermo Fisher Scientific, Shanghai, China) was used for chromatographic separation, with a column temperature of 25°C. Elution solvents consisted of 100% methanol (mobile phase B) and 5 mmol/L ammonium acetate (mobile phase C). Gradient elution (0–2 min, 90% C; 2–7 min, 90–10% C; 8–10 min, 90% C) was performed at a flow rate of 300 μL/min.

Transduction of Lentivirus

The titer of lentivirus (LV)-Cacng2-RNAi was 3×10^9 TU/ml. In vivo, penumbra injection of the lentivirus was performed as described previously. We estimated the location of the penumbra before modeling based on previous modeling experiences and references because the infarcted area of MCAO/R modeling was relatively fixed. We made a longitudinal cut (from top to bottom) approximately 2 mm from the sagittal suture through the right hemisphere, and then made a transverse diagonal cut at an approximate “2-o’clock” position to separate the core (striatum and overlying cortex) from the penumbra (adjacent

cortex). Briefly, 2 weeks before MCAO/R operation, SD rats were anesthetized and fixed in a stereotaxic apparatus (ZH-Lanxing B-type stereotaxic frame, AnhuiZhenghua Biological Equipment Co. Ltd., Anhui, China). The three injection sites were in the right hemisphere, and the stereotaxic coordinates were as follows: anteroposterior (AP) + 1.2 (site 1), 0.3 (site 2), −1.8 (site 3); mediolateral (ML) + 5.5; dorsoventral (DV) −3.5 mm from the skull. A 2-μL dose of LV was slowly infused into the penumbra at each injection site at a rate of approximately 0.5 μL/min. To avoid reflux, the needle was kept in place after injection for a further 5 min, withdrawn slightly, and then left in position for another 2 min before complete removal. Brain tissue within 2 mm of the injection site has a greater chance of being transduced with lentivirus, and the period of lentiviral expression in the brain is from 72 h to approximately 1 month after injection. At 3 h after MCAO/R, penumbral tissues were collected for further experiments. In vitro, according to the manufacturer's instructions, primary neurons were transduced with the corresponding LV (multiplicity of infection [MOI] = 10) using 20 μL HA (HitransG A, GeneChem Co., Shanghai, China) enhanced transduction solution 5–7 days after embryonic extraction. Five days after transduction, neurons were fixed with 4% paraformaldehyde. Nuclei were stained with DAPI mounting medium. Finally, sections and cells were observed using a fluorescence microscope (OLYMPUS BX50/BX-FLA/DP70) or a laser scanning confocal microscope (ZEISS LSM 880).

Intraperitoneal injection of H89

Animals were randomly assigned to one of two treatment groups comprising six or twelve animals per group: 5% dimethyl sulfoxide (DMSO; vehicle) only, or 20 mg/kg H89 in vehicle [18]. Animals were dosed twice daily on test days 0 to 2 at approximately 8:00 AM and 1:00 PM. A single dose was administered at approximately 8:30 AM on test day 3 to accommodate the 12:30 PM MCAO/R operation on day 3. At 3 h after MCAO/R, penumbral tissues were collected for further experiments. Tissue samples were stored at 80°C.

Modified Neurological Severity Score

We used the Modified Neurological Severity Score (mNSS) test, performed 24 h after reperfusion, to evaluate the MCAO/R model. The score, graded on a scale of 0–18, reflects motor, sensory, reflex, and balance functions, with higher scores indicating increased severity of neurological damage. The rats were trained and evaluated before surgery to ensure the normal baseline score of 0, and all scores were recorded by investigators who were blinded to experimental group assignment.

TTC Staining

Rats were euthanized 24 h after the MCAO/R procedure. The forebrain was extracted, frozen at −20°C for 10–20 min, and coronally dissected into 2-mm-thick slices beginning from the frontal pole. Then, the slices were immersed in TTC solution

(Nanjing Jiancheng Bioengineering Institute, Nanjing, China) at 37°C for 10–20 min. The infarct volume and total volume of each section were calculated using ImageJ software.

Rotarod Test

We used an accelerating rotarod test was used to evaluate the motor function of rats. The diameter of the rotarod spindle was 10 cm. The speed was increased from 10 to 30 rpm over 200 s, and maintained at 30 rpm for a maximum of 300 s. The time was recorded when the rat could not keep up with the speed and failed to stay on the rotarod spindle. Three rats could run simultaneously because there were two panels separating three runways, which prevented the rats from detecting each other. Three days before the test, each rat underwent training three times per day, with the final three scores recorded as the baseline. After surgery, each rat performed the test trials three times per testing day (3, 5, 7, 14), and the average of the scores was recorded as the final score for the day.

Adhesive Removal Test

The adhesive removal test was chosen to assess the sensorimotor function of the rats at 3, 5, 7, and 14 days after MCAO/R. As described in previous studies, a rat was taken out and placed in a cage for 2–3 min to familiarize it with the testing environment. An adhesive tape (2 × 3 cm) was attached to the distal region of the left and right forelimbs as a tactile stimulus. The time to contact and remove both stimuli on each forelimb was recorded in three trials per day for 3 days. After the training, any rats that were unable to contact and remove the tapes in 10 s were excluded from the experimental group. Then, all the rats received a test trial on all testing days after MCAO/R or sham surgery. Each animal was tested three times at 2-min intervals, and the final data are presented as the average time of the three tests.

Morris Water Maze

The Morris water maze test was used to examine spatial cognitive functional deficits. As previously described, a circular pool filled with opaque water was divided into four quadrants. A platform (10-cm diameter) was submerged in the pool (180-cm diameter) and maintained 2 cm under the water surface. The water temperature was maintained at 19–21°C, and the room temperature was maintained at 20–22°C. This test had two parts: a spatial learning test and a memory test. Before sham or MCAO/R surgery, the rats were trained for 3 consecutive days for the acquisition of spatial learning. Then, 22–26 days after MCAO/R, each rat was released from one of the three quadrants (except the one with the platform) and was allowed 60 s to look for the platform. Between swims, the animals were placed on the platform for 15–20 s to help them to gather the surrounding spatial cues. The average latency from three trials per day for 5 consecutive days was recorded as the final data to reflect the learning abilities of the rats. At 27 days after MCAO/R, the underwater platform was removed, and each rat was allowed to swim in the pool for 60 s from the same starting position. Spatial memory was evaluated by recording the time at which each rat crossed the site where the platform had been previously located. The swimming speed of rat was recorded on each testing day to assess the general locomotor functions of rats.

Statistical Analysis

All data are presented as the mean ± standard error of the mean (SEM). GraphPad Prism 7 was used for all statistical analyses. Differences between groups were determined using unpaired t-tests. Statistical comparisons between groups were performed using one- or two-way analysis of variance (ANOVA), and post hoc least significant difference test was used for multiple comparisons. P-values < 0.05 were considered to indicate statistical significance.

Results

Decreased D-serine Level, Increased Stargazin-SR Interaction, and Decreased Stargazin *p*T^{321} Level in the Penumbral Tissue after MCAO/R injury

To identify SR catalytic activity after MCAO/R, we established an experimental model of MCAO/R in male SD rats and subsequently performed gas/liquid chromatography analysis of brain homogenate samples from penumbral tissue. Compared with the sham group, the D-serine level was decreased at 3 h after MCAO/R and rebounded at 6 h and 24 h (Fig. 1a and b) (Sham: 1.00 ± 0.15, MCAO/R 1 h: 1.03 ± 0.17, MCAO/R 3 h: 0.79 ± 0.13, MCAO/R 6 h: 0.99 ± 0.12, MCAO/R 24 h: 1.00 ± 0.13; one-way ANOVA, $F_{(4, 25)}$ = 3.078, P < 0.05). Additionally, we used immunofluorescence labeling to determine the effects of MCAO/R on the stargazin-SR interaction. Our results indicated that the ratio of SR colocalized with stargazin was increased in the penumbral tissues of MCAO/R rats compared with that of sham rats (Fig. 1c and 1d) (Sham: 1.00 ± 0.67, MCAO/R 3 h: 1.69 ± 0.34; Student's *t* test, t (2.25) = 10, P < 0.05). The results of the co-immunoprecipitation assays consistently showed that the stargazin-SR interaction was significantly higher 3 h after MCAO/R compared with the sham group, providing further evidence for an increase in the stargazin-SR binding in the penumbral tissues of MCAO/R rats (Fig. 1e and 1f) (Sham: 1.00 ± 0.29, MCAO/R 3 h: 1.51 ± 0.38; Student's *t* test, t (2.58) = 10, P < 0.05).

It has been established that the binding between stargazin and SR is regulated by phosphorylation of stargazin at Thr-321 [17]. We therefore sought to investigate whether the stargazin *p*T^{321} level changed as a result of stroke damage. Western blotting was subsequently performed to examine the protein levels of stargazin and stargazin *p*T^{321}. Our results showed that MCAO/R 3 h increased the level of stargazin (Fig. 1g and 1i) (Sham: 1.00 ± 0.18, MCAO/R 3 h: 1.70 ± 0.09, Student's *t* test, t (8.60) = 10, P < 0.01), but it decreased the level of stargazin *p*T^{321} in the penumbrae compared with the sham group (Fig. 1h and 1j) (Sham: 1.00 ± 0.13, MCAO/R 3 h: 0.73 ± 0.09; Student's *t* test, t (4.19) = 10, P < 0.01). Thus, the ratio of stargazin *p*T^{321} to stargazin decreased by approximately 60% in the MCAO/R group (Fig. 1k) (Sham: 1.04 ± 0.3, MCAO/R 3 h: 0.43 ± 0.04, Student's *t* test, t (5.03) = 10, P < 0.01).

Genetic Knockdown of Stargazin Reduces the Stargazin-SR Interaction and Increases the D-serine Level in the Penumbral Tissue of Rats Subjected to MCAO/R

We next sought to determine whether the increases in stargazin-SR binding regulates ischemic insult. To this end, we used lentivirus-mediated expression of specific short hairpin RNAs (shRNAs) against stargazin. The transduction efficiency of stargazin lentivirus was examined by fluorescence assays *in*

vivo and *in vitro* (Fig. 2a and 2b). Then, we verified the interfering effects of the stargazin lentivirus using western blotting. Our results showed that compared with the negative control group, the level of stargazin was significantly decreased in the LV-ShRNA-STG group (Fig. 2c and 2d) (Sham: 1.00 ± 0.20, MCAO/R 3 h: 1.60 ± 0.14, MCAO/R 3 h + Ctr ShRNA: 1.64 ± 0.14, MCAO/R 3 h + ShRNA-STG: 1.06 ± 0.18, one-way ANOVA, F (3, 20) = 24.82, $P < 0.01$). Next, we examined whether the stargazin-SR interaction was affected by stargazin knockdown. The results of fluorescent labeling showed a decreased proportion of SR colocalized with stargazin in penumbral-tissue neurons of the stargazin-downregulated rats compared with those of the control rats (Fig. 2e and 2f) (MCAO/R 3 h + Ctr ShRNA: 1.00 ± 0.20, MCAO/R 3 h + ShRNA-STG: 0.57 ± 0.22, Student's *t* test, t (3.57) = 10, $P < 0.05$). Moreover, the results of the coimmunoprecipitation assay (Fig. 2g and 2h) showed a reduction in the interaction between stargazin and SR in the stargazin-downregulated group compared with that in the negative control group (MCAO/R 3 h + Ctr ShRNA: 1.00 ± 0.06, MCAO/R 3 h + ShRNA-STG: 0.75 ± 0.13; Student's *t* test, t (4.26) = 10, $P < 0.01$). We next employed gas/liquid chromatography analysis to confirm the role of the stargazin-SR interaction downregulation in SR activity. Our results showed that the level of D-serine level was increased in the stargazing-downregulated group compared with that in the negative control group (Fig. 2i and 2j) (MCAO/R 3 h + Ctr ShRNA: 1.00 ± 0.08, MCAO/R 3 h + ShRNA-STG: 1.15 ± 0.11; Student's *t* test, t (2.73) = 10, $P < 0.05$). These findings suggest that downregulation of stargazin increased the expression of D-serine, which may be associated with a reduction in the stargazin-SR interaction.

Genetic Knockdown of Stargazin Aggravates Ischemic Neuronal Death and Neurological Function after MCAO/R in Rats

Having determined that SR activity is affected by binding of stargazin to SR, we then explored whether stargazin downregulation affected neurological functions and brain damage in rats subjected to MCAO/R (Fig. 3a). Assessment of cerebral infarction 24 h after MCAO/R using TTC staining showed that total infarction volume in stargazin-knockdown rats was increased compared with the control rats (Fig. 3b and 3c) (MCAO/R 24 h: 0.27 ± 0.07, MCAO/R 24 h + Ctr ShRNA: 0.27 ± 0.06, MCAO/R 24 h + ShRNA-STG: 0.36 ± 0.03; one-way ANOVA, $F_{(2, 15)} = 7.592$, $P < 0.05$). Furthermore, mNSS was significantly higher in the stargazing-downregulated group compared with the negative control group (Fig. 3d) (Sham: 0.00 ± 0.00, MCAO/R 24 h: 9.67 ± 2.65, MCAO/R 24 h + Ctr ShRNA: 10.10 ± 2.33, MCAO/R 24 h + ShRNA-STG: 14.25 ± 2.61; one-way ANOVA, $F_{(3, 34)} = 80.72$, $P < 0.0001$). To further evaluate the functional-recovery effect of stargazin downregulation in rats subjected to MCAO/R, we used the rotarod test to assess the post-stroke locomotor activity, the adhesive-removal test to evaluate forelimb sensorimotor asymmetries, and the Morris water maze test to examine the spatial learning and memory function. Untreated MCAO/R rats performed significantly worse in all three tests compared with the sham-treated rats (Fig. 3e–3k). Moreover, rats treated with shRNA-stargazin showed a significant increase in the time spent on the accelerating rotarod compared with the MCAO/R +LV-shRNA-control rats (Fig. 3e) (ShRNA-STG [$F_{(3, 196)} = 204.00$, $P < 0.0001$], test day [$F_{(4, 196)} = 124.20$, $P < 0.0001$], with an interaction observed between these two factors [$F_{(12, 196)} = 16.63$, $P < 0.0001$]). The sensorimotor function was aggravated in MCAO/R + LV-shRNA-stargazin rats compared with that of the MCAO/R+LV-shRNA-control rats, as demonstrated by the

significantly shortened contact time (Fig. 3f) (ShRNA-STG [$F_{(3, 196)}$ = 101.00, P < 0.0001], test day [$F_{(4, 196)}$ = 91.86, P < 0.0001], with an interaction observed between these two factors [$F_{(12, 196)}$ = 11.12, P < 0.0001]) and removal time (Fig. 3g) (ShRNA-STG ($F_{(3, 196)}$ = 140.10, P < 0.0001), test day ($F_{(4, 196)}$ = 128.90, P < 0.0001), with an interaction observed between these two factors ($F_{(12, 196)}$ = 15.70, P < 0.0001]). The Morris water maze test, performed 22 to 27 days post-MCAO/R (Fig. 3a), showed that stargazin downregulation aggravated spatial learning, as evidenced by the decreased time spent seeking out the underwater hidden platform compared with the time taken by the lentivirus-negative control rats (Fig. 3h and 3i) (ShRNA-STG [$F_{(3, 190)}$ = 29.64, P < 0.0001], test day [$F_{(4, 190)}$ = 21.37, P < 0.0001], with an interaction observed between these two factors ($F_{(12, 190)}$ = 0.21, P = 1.00]). Unlike the other tests used in our study, the memory test indicated no difference in memory function between the MCAO/R +LV-shRNA-stargazin group and the MCAO/R + LV-shRNA-control group. Additionally, the swimming speed was similar among the rats used in our present study (Fig. 3j) (Sham: 27.04 ± 4.35, MCAO/R: 27.59 ± 3.04, MCAO/R + Ctr ShRNA: 27.32 ± 4.06, MCAO/R + ShRNA-STG: 27.11 ± 5.68; one-way ANOVA, $F_{(3, 37)}$ = 0.03, P = 0.99). On day 27 after sham or MCAO/R surgery, the platform was removed and the rats were evaluated using the memory test. Compared with the performance of the rats in the sham group, the rats in the MCAO/R group showed a spatial memory deficit, as demonstrated by a reduced numbers of passes over the previous location of the platform (Fig. 3k) (Sham: 2.42 ± 1.00, MCAO/R: 1.30 ± 0.95, MCAO/R + Ctr ShRNA: 1.18 ± 0.75, MCAO/R + ShRNA-STG: 1.11 ± 0.78; one-way ANOVA, $F_{(3, 38)}$ = 5.52, P < 0.05). These results indicated that downregulation of stargazin aggravated stroke outcomes, which may be associated with increased expression of D-serine regulated by stargazin-SR interaction.

Inhibition of Phosphorylation of Stargazin-Thr-321 Increases Stargazin-SR Interaction and Decreases D-serine Expression in Penumbral Tissue of Rats Subjected to MCAO/R

It has been reported that the interaction between stargazin and PSD-95 is inhibited by phosphorylation of stargazin at Thr-321[19]. It also has been demonstrated that mutation of stargazin-Thr-321 to aspartate or glutamate, mimicking phosphorylation, abolishes binding to SR [17]. Moreover, the stargazin C terminus contains a consensus sequence for phosphorylation by cAMP-dependent protein kinase A (PKA) [17]. Thus, we used H89, an inhibitor of PKA, to inhibit the phosphorylation of stargazin-Thr-321 and to determine whether this inhibition affected the stargazin-SR interaction and expression of D-serine. We intraperitoneally injected H89 in MCAO/R rats. The increased level of stargazin in penumbrae was unchanged in the MCAO/R 3 h + H89 group compared with those of the MCAO/R 3 h + DMSO group (Fig. 4a and 4c) (MCAO/R 3 h + DMSO: 1.01 ± 0.32, MCAO/R 3 h + H89: 1.43 ± 0.15; Student's t test, t (2.93) = 10, P < 0.05); however, the level of phosphorylation of stargazin-Thr-321 in the penumbrae was significantly decreased in the MCAO/R 3 h + H89 group compared with the MCAO/R 3 h + DMSO group (Fig. 4b and 4d) (MCAO/R 3 h + DMSO: 1.00 ± 0.12, MCAO/R 3 h + H89: 0.78 ± 0.12; Student's t test, t (3.14) = 10, P < 0.05). The ratio of stargazin $p\mathrm{T}^{321}$ to stargazin also decreased in the MCAO/R group (MCAO/R 3 h + DMSO: 1.10 ± 0.42, MCAO/R 3 h + H89: 0.55 ± 0.12; Student's t test, t (3.07) = 10, P < 0.05). Next, we used fluorescent labeling to investigate whether the stargazin-SR interaction is inhibited by H89. The results showed an increased proportion of SR colocalized with stargazin in penumbral-tissue

neurons of the MCAO/R 3 h + H89 rats compared to that of the MCAO/R 3 h + DMSO rats (Fig. 4f and g) (MCAO/R 3 h + DMSO: 0.66 ± 0.40, MCAO/R 3 h + H89: 1.25 ± 0.39, Student's *t* test, t (2.63) = 10, $P < 0.05$). Additionally, a coimmunoprecipitation assay was used to analyze the brain-tissue homogenates from H89-treated and DMSO-treated rats to determine whether the protein levels of phosphorylation of stargazin-Thr-321 affected the interaction between stargazin and SR. As shown in Fig. 4h and 4i, increased interaction between stargazin and SR was observed in the MCAO/R 3 h + H89 group compared with those in the MCAO/R 3 h + DMSO group (MCAO/R 3 h + DMSO: 1.00 ± 0.35, MCAO/R 3 h + H89: 2.10 ± 0.69; Student's *t* test, t (3.47) = 10, $P < 0.01$). Moreover, decreased D-serine was observed in the MCAO/R 3 h + H89 group compared with that in the MCAO/R 3 h + DMSO group (Fig. 4j and 4k) (MCAO/R 3 h + DMSO: 1.00 ± 0.14, MCAO/R 3 h + H89: 0.75 ± 0.06, Student's *t* test, t (4.01) = 10, $P < 0.01$). These findings suggested that inhibition of stargazin-Thr-321 phosphorylation decreased the expression of D-serine, which might be associated with increased stargazin-SR interaction.

Inhibition of Stargazin-Thr-321 Phosphorylation Protects Against Ischemic Neuronal Death and Improves Neurological Function after MCAO/R in Rats

We then investigated whether the inhibition of stargazin-Thr-321 phosphorylation affected neurological functions and brain damage in rats subjected to MCAO/R (Fig. 5a). Assessment of cerebral infarction 24 h after MCAO/R using TTC staining and mNSS score showed that total infarction volume in H89-treated rats was reduced compared with that in the DMSO-treated rats (Fig. 5b and 5c) (MCAO/R 3 h + DMSO: 25.17 ± 3.51, MCAO/R 3 h + H89: 15.59 ± 5.85, Student's *t* test, t (3.44) = 10, $P < 0.01$). Furthermore, mNSS was significantly lower in the MCAO/R + H89 group than in the MCAO/R +DMSO group (Fig. 5d) (MCAO/R 3 h + DMSO: 8.67 ± 2.00, MCAO/R 3 h + H89: 6.11 ± 2.26, Student's *t* test, t (2.54) = 16, $P < 0.05$). To further evaluate the functional recovery effect of the inhibition of stargazin-Thr-321 phosphorylation in rats subjected to MCAO/R, we used the rotarod test to assess the post-stroke locomotor activity, the adhesive-removal test to evaluate forelimb sensorimotor asymmetries, and the Morris water maze test to examine the spatial learning and memory function. Rats treated with H89 showed a significant increase in the time spent on the accelerating rotarod compared with that of DMSO-treated rats (Fig. 5e) (H89 [$F_{(1, 94)} = 10.08$, $P < 0.01$], test day [$F_{(4, 94)} = 55.49$, $P < 0.0001$], with an interaction observed between these two factors [$F_{(4, 94)} = 0.75$, $P = 0.56$]). Moreover, the sensorimotor function was improved in MCAO/R + H89 rats compared with that of the MCAO/R + DMSO rats, as demonstrated by a significantly shortened contact time (Fig. 5f) (H89 [$F_{(1, 94)} = 5.36$, $P < 0.05$], test day [$F_{(4, 94)} = 24.21$, $P < 0.0001$], with an interaction observed between these two factors [$F_{(4, 94)} = 0.50$, $P = 0.73$]) and removal time (Fig. 5g) (H89 [$F_{(1, 94)} = 8.59$, $P < 0.01$], test day [$F_{(4, 94)} = 40.91$, $P < 0.0001$], with an interaction observed between these two factors [$F_{(4, 94)} = 0.96$, $P = 0.43$]). The Morris water maze test, performed 22 to 27 days post-MCAO/R (Fig. 5a), showed that H89-treated rats rescued spatial learning, as evidenced by the decreased time spent seeking out the underwater hidden platform compared with that of the DMSO-treated rats (Fig. 5h and 5i) (H89 [$F_{(1, 90)} = 12.53$, $P < 0.05$], test day [$F_{(4, 90)} = 19.81$, $P < 0.0001$], with an interaction observed between these two factors [$F_{(4, 90)} = 0.29$, $P = 0.88$]). Unlike the other tests used in our study, the memory test indicated no significant difference in memory function

between the MCAO/R + H89 group and the MCAO/R + DMSO group (Fig. 5k) (MCAO/R 3 h + DMSO: 1.30 ± 0.82, MCAO/R 3 h + H89: 1.60 ± 0.70; Student's *t* test, t (0.88) = 18, *P* = 0.39). Additionally, the swimming speed was similar among the rats used in our study (Fig. 5j) (MCAO/R 3 h + DMSO: 28.25 ± 4.39, MCAO/R 3 h + H89: 28.04 ± 3.32, Student's *t* test, t (0.13) = 18, *P* = 0.90). These results indicated that the inhibition of stargazin-Thr-321 phosphorylation improved stroke outcomes, which may be associated with decreased expression of D-serine regulated by stargazin-SR interaction.

Discussion

Our study has provided two key findings. First, MCAO/R increased the stargazin-SR interaction and reduced the D-serine expression in penumbral tissue, which is associated with a low phosphorylation level of stargazin-Thr-321. Second, inhibition or further promotion of stargazin-SR interaction enhanced or attenuated D-serine expression, ischemic neuronal death, and neurobehavioral deficits. Collectively, these results suggested that enhanced stargazin-SR interaction in penumbral tissue in MCAO/R rats served as a protective mechanism in the context of cerebral ischemia/reperfusion injury.

In the past 20 years, the NMDA receptor has become the major focus of studies for treating stroke [20-24]. Activation of NMDA receptors is considered to be a primary cause of excitotoxicity in ischemic insult as a result of its high permeability to Ca^{2+} [25]. Opening of the NMDA receptor channels requires the activation of two distinct compulsory co-agonist binding sites, one that binds glutamate and the other that binds glycine or D-serine [26,9]. During brain ischemia, D-serine release could potentiate excitotoxic actions of glutamate acting at NMDA receptors [26]. Degrading endogenous D-serine by D-amino acid oxidase (DAAOX), an enzyme that efficiently degrades extracellular D-serine, protects neurons from damage induced by simulated ischemia [27]. SR deletion mice, in which D-serine levels are reduced by 90%, have diminished neurotoxicity following MCAO [10]. Nevertheless, these results suggest only that endogenous D-serine is required for NMDA receptor-mediated excitotoxicity, but they do not demonstrate that increased D-serine is released during ischemia. In this study, we used gas/liquid chromatography analysis to detect endogenous D-serine levels at multiple time points after MCAO/R. Our data showed that the D-serine levels significantly reduced in the 3 h after MCAO/R, and subsequently returned to normal levels 6 and 24 h after MCAO/R. D-serine has a half-life of nearly 17 h, indicating slow metabolism in the brain [28]. The D-serine levels decreased only 3 h after stroke onset in the present study, suggesting the inhibition of SR activity. One of the main questions arising from this study is how SR activity becomes inhibited in response to cerebral ischemic insult. SR catalytic activity is thought to be controlled by multiple mechanisms. For instance, NMDAR activation triggers the production of nitric oxide (NO), which leads to the S-nitrosylation of SR and inhibition of SR activity [15]. SR is physiologically inhibited by PIP2 [14] and binds to stargazin, which also inhibits its activity [17]. In this study, we showed increased expression levels of stargazin and its interaction with SR in the penumbra. We also demonstrated that stargazin becomes dephosphorylated at pT321 in cortical neurons following ischemic insult. Some studies have indicated that the stargazin C terminus contains a sequence for phosphorylation by cAMP-dependent protein kinase A (PKA). Meanwhile, it has been shown that the

stargazin C terminus is phosphorylated at the Thr-321 residue [19], and the binding between stargazin and SR is inhibited by phosphorylation of stargazin at Thr-321 [17]. Our results showed that the application of the PKA inhibitor H89 promoted stargazin dephosphorylation at pT321, augmented the stargazin-SR interaction, and inactivated SR. Additionally, H89 protected against ischemic neuronal death and improved neurological function. Indeed, our data suggested that the PKA inhibitor H89 reduced brain infarction and improved neurological functions as a result of dephosphorylation of $p\mathrm{T}^{321}$, which allowed stargazin to bind and inactivate SR. However, some studies have found the protective effects of H89 on cerebral ischemia, which might be not related to the inhibition of PKA. It has been reported that H89 may contribute to brain recovery after ischemic stroke by regulating proteins related to neuronal apoptosis and synaptic plasticity [29]. Thus, H89 confers protection from brain damage in many aspects of nervous system function. Conversely, several reports have shown that the effects of some neuroprotective agents are eliminated by H89 intervention [30-32]. One explanation for these findings is that these neuroprotective agents protect neurons against ischemia through the cAMP/PKA/CREB signaling pathways, promote the phosphorylation of p-CREB, and play important anti-apoptotic roles. The mutation of stargazin-Thr-321 to alanine, which mimics dephosphorylation and augments stargazin-SR binding, are needed in the future research because pharmacological methods are nonspecific.

We next silenced the stargazin gene to determine the effects of separating the stargazin-SR interaction on cerebral ischemic insult. Our data showed that downregulating the expression of stargazin increased MCAO/R insult to cortical neuronal cells and aggravated neurological function; the mechanism driving these events may be associated with the decreased stargazin-SR interaction and the increased expression of D-serine. Stargazin is a 40-kDa neuronal transmembrane protein that controls the surface and synaptic expression of AMPARs [33-38]. S-nitrosylation of stargazin increases interaction with the AMPAR subunit GluA1, resulting in increased surface expression of AMPARs [39]. Although we directly demonstrated that stargazin knockdown increased SR activity and reduced stargazin-SR binding, we did not examine the influence of stargazin knockdown on AMPAR surface expression because the regulation of stargazin to AMPAR surface expression was nNOS dependent [39] and cerebral ischemia reduced nNOS expression [40]. Thus, it would not be possible that increased AMPAR surface expression is mediated by stargazin following cerebral ischemic insult. In addition, stargazin has been reported to bind to PSD95, AP-2, and AP-3A to regulate NMDA-induced AMPA receptor trafficking [19,41]. Thus, directly silencing stargazin can cause severe side effects. Although previous studies have identified the first 66 N-terminal amino acids of SR as critical fragments for stargazin binding, the key binding sites between stargazin and SR remain to be determined [17]. It is possible to develop a small-molecular inhibitor or generate a cell membrane permeable peptide to specifically disturb the stargazin-SR interaction. Therefore, further studies are warranted to clarify whether stargazin-SR binding is involved in the various forms of AMPA receptor trafficking.

In summary, our results showed that under ischemic insult, stargazin was dephosphorylated at $p\mathrm{T}^{321}$ and could bind to SR to inhibit SR activity, resulting in a decrease in D-serine release(Fig 6). Thus,

dephosphorylated stargazin at pT^{321} can be considered to be a protective mechanism against brain damage in stroke.

Declarations

Disclosures: This study was supported by the National Science Foundation of China (No. 81803553, 82071300, 82171282); the Natural Scientific Foundation of Jiangsu Province (No. BK20160351); the National Key R&D Program of Jiangsu Province (Social Development) (key project: Clinical Frontier Technology) (BE2019666); and Open Project of Jiangsu Key Laboratory of Major Neuropsychiatric Diseases (KJS2031). All authors declare that there are no conflicts of interest.

Data Availability

Data that support the findings of this study are available from the corresponding author upon request.

Acknowledgments

We thank LetPub (www.letpub.com) for its linguistic assistance during the preparation of this manuscript.

References

1. Feigin VL, Norrving B, Mensah GA (2017) Global Burden of Stroke. Circulation research 120(3):439–448. doi:10.1161/CIRCRESAHA.116.308413
2. Fossati M, Charrier C (2021) Trans-synaptic interactions of ionotropic glutamate receptors. Curr Opin Neurobiol 66:85–92. doi:10.1016/j.conb.2020.09.001
3. Pagano J, Giona F, Beretta S, Verpelli C, Sala C (2021) N-methyl-d-aspartate receptor function in neuronal and synaptic development and signaling. Curr Opin Pharmacol 56:93–101. doi:10.1016/j.coph.2020.12.006
4. Drejer J, Benveniste H, Diemer NH, Schousboe A (1985) Cellular origin of ischemia-induced glutamate release from brain tissue in vivo and in vitro. Journal of neurochemistry 45(1):145–151. doi:10.1111/j.1471-4159.1985.tb05486.x
5. Rossi DJ, Oshima T, Attwell D (2000) Glutamate release in severe brain ischaemia is mainly by reversed uptake. Nature 403(6767):316–321. doi:10.1038/35002090
6. Lipton SA (2006) Paradigm shift in neuroprotection by NMDA receptor blockade: memantine and beyond. Nature reviews Drug discovery 5(2):160–170. doi:10.1038/nrd1958
7. Lo EH, Dalkara T, Moskowitz MA (2003) Mechanisms, challenges and opportunities in stroke. Nature reviews Neuroscience 4(5):399–415. doi:10.1038/nrn1106
8. Oliet SH, Mothet JP (2006) Molecular determinants of D-serine-mediated gliotransmission: from release to function. Glia 54(7):726–737. doi:10.1002/glia.20356

9. Wolosker H (2006) D-serine regulation of NMDA receptor activity. Science's STKE: signal transduction knowledge environment 2006 (356):pe41. doi:10.1126/stke.3562006pe41
10. Mustafa AK, Ahmad AS, Zeynalov E, Gazi SK, Sikka G, Ehmsen JT, Barrow RK, Coyle JT, Snyder SH, Dore S (2010) Serine racemase deletion protects against cerebral ischemia and excitotoxicity. The Journal of neuroscience: the official journal of the Society for Neuroscience 30(4):1413–1416. doi:10.1523/JNEUROSCI.4297-09.2010
11. Fujii K, Maeda K, Hikida T, Mustafa AK, Balkissoon R, Xia J, Yamada T, Ozeki Y, Kawahara R, Okawa M, Huganir RL, Ujike H, Snyder SH, Sawa A (2006) Serine racemase binds to PICK1: potential relevance to schizophrenia. Molecular psychiatry 11(2):150–157. doi:10.1038/sj.mp.4001776
12. Hikida T, Mustafa AK, Maeda K, Fujii K, Barrow RK, Saleh M, Huganir RL, Snyder SH, Hashimoto K, Sawa A (2008) Modulation of D-serine levels in brains of mice lacking PICK1. Biol Psychiatry 63(10):997–1000. doi:10.1016/j.biopsych.2007.09.025
13. Kim PM, Aizawa H, Kim PS, Huang AS, Wickramasinghe SR, Kashani AH, Barrow RK, Huganir RL, Ghosh A, Snyder SH (2005) Serine racemase: activation by glutamate neurotransmission via glutamate receptor interacting protein and mediation of neuronal migration. Proc Natl Acad Sci USA 102(6):2105–2110. doi:10.1073/pnas.0409723102
14. Mustafa AK, van Rossum DB, Patterson RL, Maag D, Ehmsen JT, Gazi SK, Chakraborty A, Barrow RK, Amzel LM, Snyder SH (2009) Glutamatergic regulation of serine racemase via reversal of PIP2 inhibition. Proc Natl Acad Sci USA 106(8):2921–2926. doi:10.1073/pnas.0813105106
15. Mustafa AK, Kumar M, Selvakumar B, Ho GP, Ehmsen JT, Barrow RK, Amzel LM, Snyder SH (2007) Nitric oxide S-nitrosylates serine racemase, mediating feedback inhibition of D-serine formation. Proc Natl Acad Sci USA 104(8):2950–2955. doi:10.1073/pnas.0611620104
16. Bats C, Groc L, Choquet D (2007) The interaction between Stargazin and PSD-95 regulates AMPA receptor surface trafficking. Neuron 53(5):719–734. doi:10.1016/j.neuron.2007.01.030
17. Ma TM, Paul BD, Fu C, Hu S, Zhu H, Blackshaw S, Wolosker H, Snyder SH (2014) Serine racemase regulated by binding to stargazin and PSD-95: potential N-methyl-D-aspartate-alpha-amino-3-hydroxy-5-methyl-4-isoxazolepropionic acid (NMDA-AMPA) glutamate neurotransmission cross-talk. J Biol Chem 289(43):29631–29641. doi:10.1074/jbc.M114.571604
18. Davis MA, Hinerfeld D, Joseph S, Hui YH, Huang NH, Leszyk J, Rutherford-Bethard J, Tam SW (2006) Proteomic analysis of rat liver phosphoproteins after treatment with protein kinase inhibitor H89 (N-(2-[p-bromocinnamylamino-]ethyl)-5-isoquinolinesulfonamide). J Pharmacol Exp Ther 318(2):589–595. doi:10.1124/jpet.105.100032
19. Choi J, Ko J, Park E, Lee JR, Yoon J, Lim S, Kim E (2002) Phosphorylation of stargazin by protein kinase A regulates its interaction with PSD-95. J Biol Chem 277(14):12359–12363. doi:10.1074/jbc.M200528200
20. Hardingham GE, Fukunaga Y, Bading H (2002) Extrasynaptic NMDARs oppose synaptic NMDARs by triggering CREB shut-off and cell death pathways. Nature neuroscience 5(5):405–414. doi:10.1038/nn835

21. Cook DJ, Teves L, Tymianski M (2012) Treatment of stroke with a PSD-95 inhibitor in the gyrencephalic primate brain. Nature 483(7388):213–217. doi:10.1038/nature10841
22. Hill MD, Martin RH, Mikulis D, Wong JH, Silver FL, Terbrugge KG, Milot G, Clark WM, Macdonald RL, Kelly ME, Boulton M, Fleetwood I, McDougall C, Gunnarsson T, Chow M, Lum C, Dodd R, Poublanc J, Krings T, Demchuk AM, Goyal M, Anderson R, Bishop J, Garman D, Tymianski M, investigators Et (2012) Safety and efficacy of NA-1 in patients with iatrogenic stroke after endovascular aneurysm repair (ENACT): a phase 2, randomised, double-blind, placebo-controlled trial. The Lancet Neurology 11 (11):942-950. doi:10.1016/S1474-4422(12)70225-9
23. Hill MD, Goyal M, Menon BK, Nogueira RG, McTaggart RA, Demchuk AM, Poppe AY, Buck BH, Field TS, Dowlatshahi D, van Adel BA, Swartz RH, Shah RA, Sauvageau E, Zerna C, Ospel JM, Joshi M, Almekhlafi MA, Ryckborst KJ, Lowerison MW, Heard K, Garman D, Haussen D, Cutting SM, Coutts SB, Roy D, Rempel JL, Rohr AC, Iancu D, Sahlas DJ, Yu AYX, Devlin TG, Hanel RA, Puetz V, Silver FL, Campbell BCV, Chapot R, Teitelbaum J, Mandzia JL, Kleinig TJ, Turkel-Parrella D, Heck D, Kelly ME, Bharatha A, Bang OY, Jadhav A, Gupta R, Frei DF, Tarpley JW, McDougall CG, Holmin S, Rha JH, Puri AS, Camden MC, Thomalla G, Choe H, Phillips SJ, Schindler JL, Thornton J, Nagel S, Heo JH, Sohn SI, Psychogios MN, Budzik RF, Starkman S, Martin CO, Burns PA, Murphy S, Lopez GA, English J, Tymianski M, Investigators E-N (2020) Efficacy and safety of nerinetide for the treatment of acute ischaemic stroke (ESCAPE-NA1): a multicentre, double-blind, randomised controlled trial. Lancet 395(10227):878–887. doi:10.1016/S0140-6736(20)30258-0
24. Tu W, Xu X, Peng L, Zhong X, Zhang W, Soundarapandian MM, Balel C, Wang M, Jia N, Zhang W, Lew F, Chan SL, Chen Y, Lu Y (2010) DAPK1 interaction with NMDA receptor NR2B subunits mediates brain damage in stroke. Cell 140(2):222–234. doi:10.1016/j.cell.2009.12.055
25. Rossi DJ, Brady JD, Mohr C (2007) Astrocyte metabolism and signaling during brain ischemia. Nature neuroscience 10(11):1377–1386. doi:10.1038/nn2004
26. Martineau M, Baux G, Mothet JP (2006) D-serine signalling in the brain: friend and foe. Trends in neurosciences 29(8):481–491. doi:10.1016/j.tins.2006.06.008
27. Katsuki H, Nonaka M, Shirakawa H, Kume T, Akaike A (2004) Endogenous D-serine is involved in induction of neuronal death by N-methyl-D-aspartate and simulated ischemia in rat cerebrocortical slices. J Pharmacol Exp Ther 311(2):836–844. doi:10.1124/jpet.104.070912
28. Dunlop DS, Neidle A (1997) The origin and turnover of D-serine in brain. Biochem Biophys Res Commun 235(1):26–30. doi:10.1006/bbrc.1997.6724
29. Song J, Cheon SY, Lee WT, Park KA, Lee JE (2015) PKA Inhibitor H89 (N-[2-p-bromocinnamylamino-ethyl]-5-isoquinolinesulfonamide) Attenuates Synaptic Dysfunction and Neuronal Cell Death following Ischemic Injury. Neural plasticity 2015:374520. doi:10.1155/2015/374520
30. Gao X, Zhang X, Cui L, Chen R, Zhang C, Xue J, Zhang L, He W, Li J, Wei S, Wei M, Cui H (2020) Ginsenoside Rb1 Promotes Motor Functional Recovery and Axonal Regeneration in Post-stroke Mice through cAMP/PKA/CREB Signaling Pathway. Brain research bulletin 154:51–60. doi:10.1016/j.brainresbull.2019.10.006

31. Wang MD, Huang Y, Zhang GP, Mao L, Xia YP, Mei YW, Hu B (2012) Exendin-4 improved rat cortical neuron survival under oxygen/glucose deprivation through PKA pathway. Neuroscience 226:388–396. doi:10.1016/j.neuroscience.2012.09.025
32. Zhang D, Jin W, Liu H, Liang T, Peng Y, Zhang J, Zhang Y (2020) ENT1 inhibition attenuates apoptosis by activation of cAMP/pCREB/Bcl2 pathway after MCAO in rats. Exp Neurol 331:113362. doi:10.1016/j.expneurol.2020.113362
33. Letts VA, Felix R, Biddlecome GH, Arikkath J, Mahaffey CL, Valenzuela A, Bartlett FS 2nd, Mori Y, Campbell KP, Frankel WN (1998) The mouse stargazer gene encodes a neuronal Ca2+-channel gamma subunit. Nat Genet 19(4):340–347. doi:10.1038/1228
34. Tomita S, Chen L, Kawasaki Y, Petralia RS, Wenthold RJ, Nicoll RA, Bredt DS (2003) Functional studies and distribution define a family of transmembrane AMPA receptor regulatory proteins. J Cell Biol 161(4):805–816. doi:10.1083/jcb.200212116
35. Vandenberghe W, Nicoll RA, Bredt DS (2005) Stargazin is an AMPA receptor auxiliary subunit. Proc Natl Acad Sci USA 102(2):485–490. doi:10.1073/pnas.0408269102
36. Nicoll RA, Tomita S, Bredt DS (2006) Auxiliary subunits assist AMPA-type glutamate receptors. Science 311(5765):1253–1256. doi:10.1126/science.1123339
37. Stein EL, Chetkovich DM (2010) Regulation of stargazin synaptic trafficking by C-terminal PDZ ligand phosphorylation in bidirectional synaptic plasticity. Journal of neurochemistry 113(1):42–53. doi:10.1111/j.1471-4159.2009.06529.x
38. Ben-Yaacov A, Gillor M, Haham T, Parsai A, Qneibi M, Stern-Bach Y (2017) Molecular Mechanism of AMPA Receptor Modulation by TARP/Stargazin. Neuron 93 (5):1126-1137 e1124. doi:10.1016/j.neuron.2017.01.032
39. Selvakumar B, Huganir RL, Snyder SH (2009) S-nitrosylation of stargazin regulates surface expression of AMPA-glutamate neurotransmitter receptors. Proc Natl Acad Sci USA 106(38):16440–16445. doi:10.1073/pnas.0908949106
40. Zhou L, Li F, Xu HB, Luo CX, Wu HY, Zhu MM, Lu W, Ji X, Zhou QG, Zhu DY (2010) Treatment of cerebral ischemia by disrupting ischemia-induced interaction of nNOS with PSD-95. Nature medicine 16(12):1439–1443. doi:10.1038/nm.2245
41. Matsuda S, Kakegawa W, Budisantoso T, Nomura T, Kohda K, Yuzaki M (2013) Stargazin regulates AMPA receptor trafficking through adaptor protein complexes during long-term depression. Nature communications 4:2759. doi:10.1038/ncomms3759

Figures

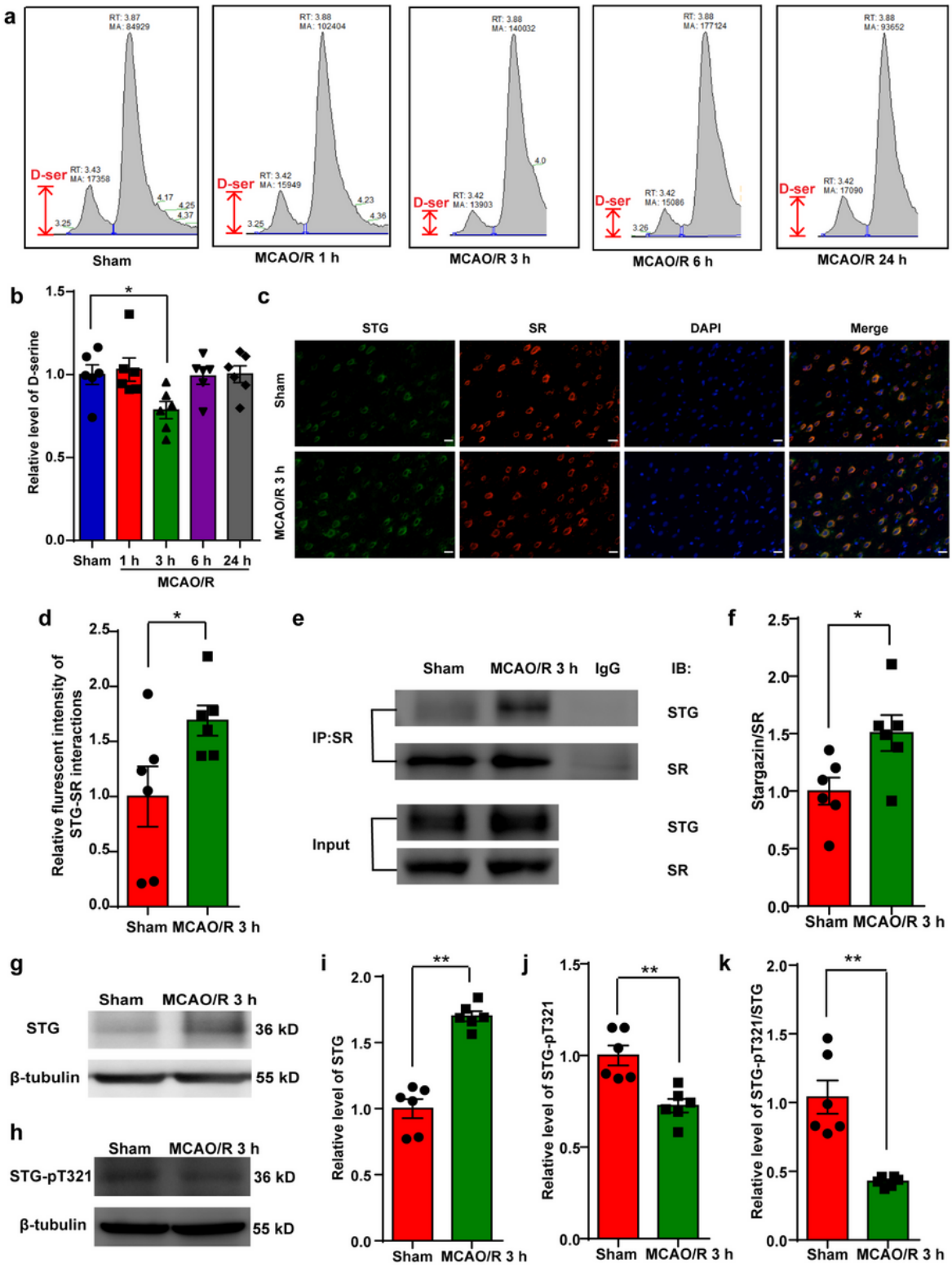

Figure 1

D-serine (D-ser) level, stargazin (STG)-serine racemase (SR) interaction, and phosphorylation level of stargazin-Thr-321 (STG-pT321) in the ischemic penumbra of MCAO/R rats. a–b. Gas/liquid chromatography analysis and quantification of D-serine in the ischemic penumbra. (*P < 0.05 vs. sham, n = 6 per group). c–d. Double immunofluorescence analysis was performed using antibodies against stargazin (green) and SR (red) in brain sections. Nuclei were fluorescently labeled with DAPI (blue).

Merged images show increased colocalization of stargazin and SR at 3 hours (h) after MCAO/R (*P < 0.05 vs. sham, n = 6 per group). Scale bar: 20 μm. e–f. Coimmunoprecipitation and quantification of the interaction level of stargazin-SR in the ischemic penumbra (*P < 0.05 vs. sham, n = 6 per group). g–k. Western blotting of stargazin and phosphorylation of stargazin-Thr-321 in the ischemic penumbra of sham and MCAO/R rats (**P < 0.01 vs. sham, n = 6 per group). All data are presented as the mean ± SEM.

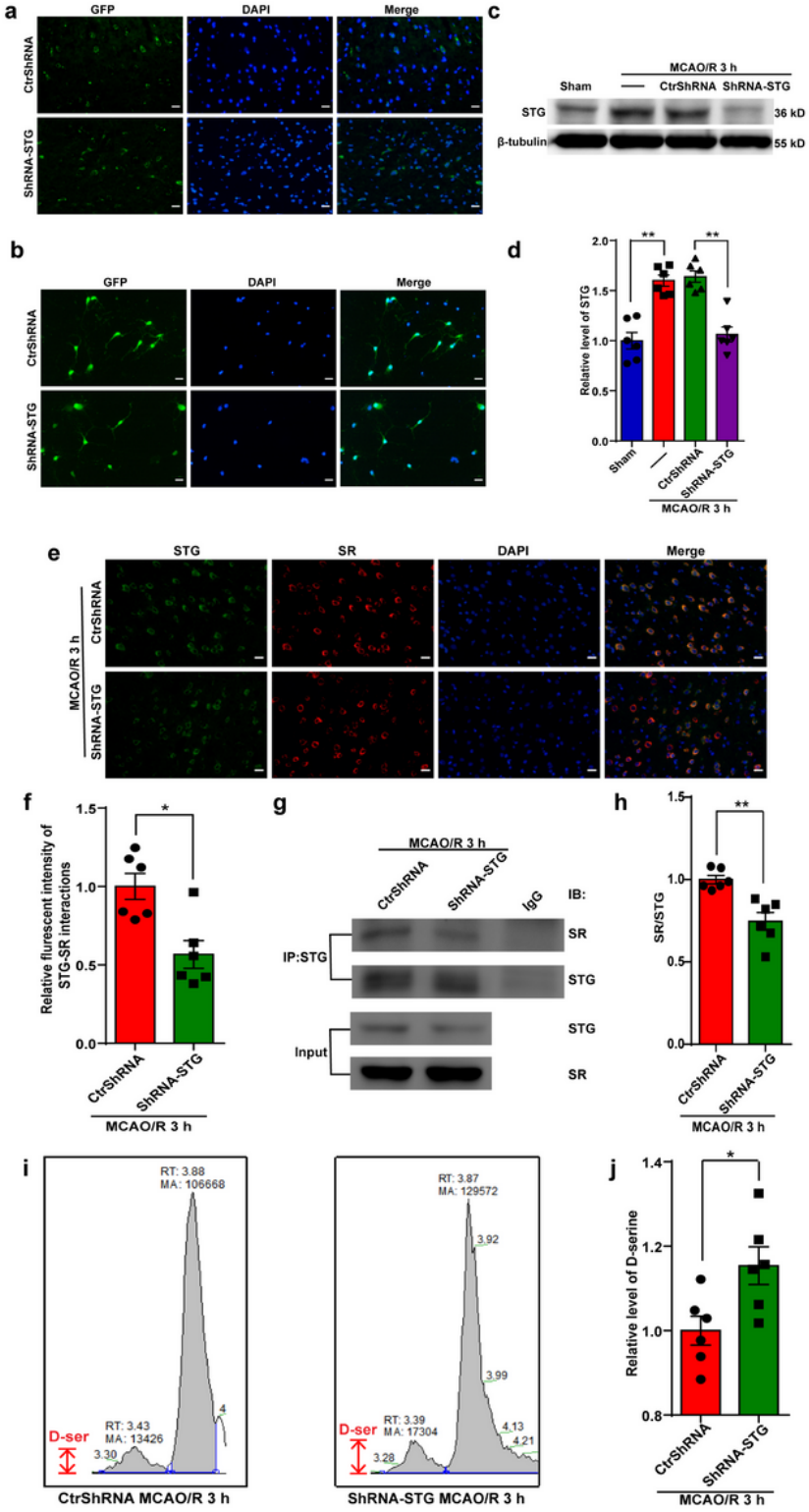

Figure 2

Effects of genetic knockdown of stargazin (STG) on the stargazin- serine racemase (SR) interaction and D-serine (D-ser) level. a–b. Immunofluorescence analysis of transfection efficiency in brain sections and neurons. Scale bar: 20 μm. c–d. Western blot analysis of the transduction efficiency and stargazin protein level in the ischemic penumbra 3 hours (h) after MCAO/R. (MCAO/R 3 h vs. sham, **P < 0.01; MCAO/R 3 h + ShRNA-STG vs. MCAO/R 3 h + CtrShRNA; **P < 0.01; n = 6 per group). e. Double immunofluorescence analysis was performed with antibodies against stargazin (green) and SR (red) in brain sections. Nuclei were fluorescently labeled with DAPI (blue). Merged images show decrease colocalization of stargazin and SR in the ischemic penumbra of MCAO/R rats after stargazin knockdown. Scale bar: 20 μm. f. The relative fluorescent intensity of the stargazin-SR interaction in the ischemic penumbra (*P < 0.05 vs. MCAO/R 3 h + CtrShRNA, n = 6 per group). g–h. Coimmunoprecipitation and quantification of the interaction level of stargazin and SR in the ischemic penumbra of MCAO/R rats after stargazin knockdown (**P < 0.01 vs. MCAO/R 3 h + CtrShRNA, n = 6 per group). i–j. Gas/liquid chromatography analysis and quantification of D-serine in the ischemic penumbra of MCAO/R rats after stargazin knockdown (*P < 0.05 vs. MCAO/R 3 h, n = 6 per group). All data are presented as the mean ± SEM.

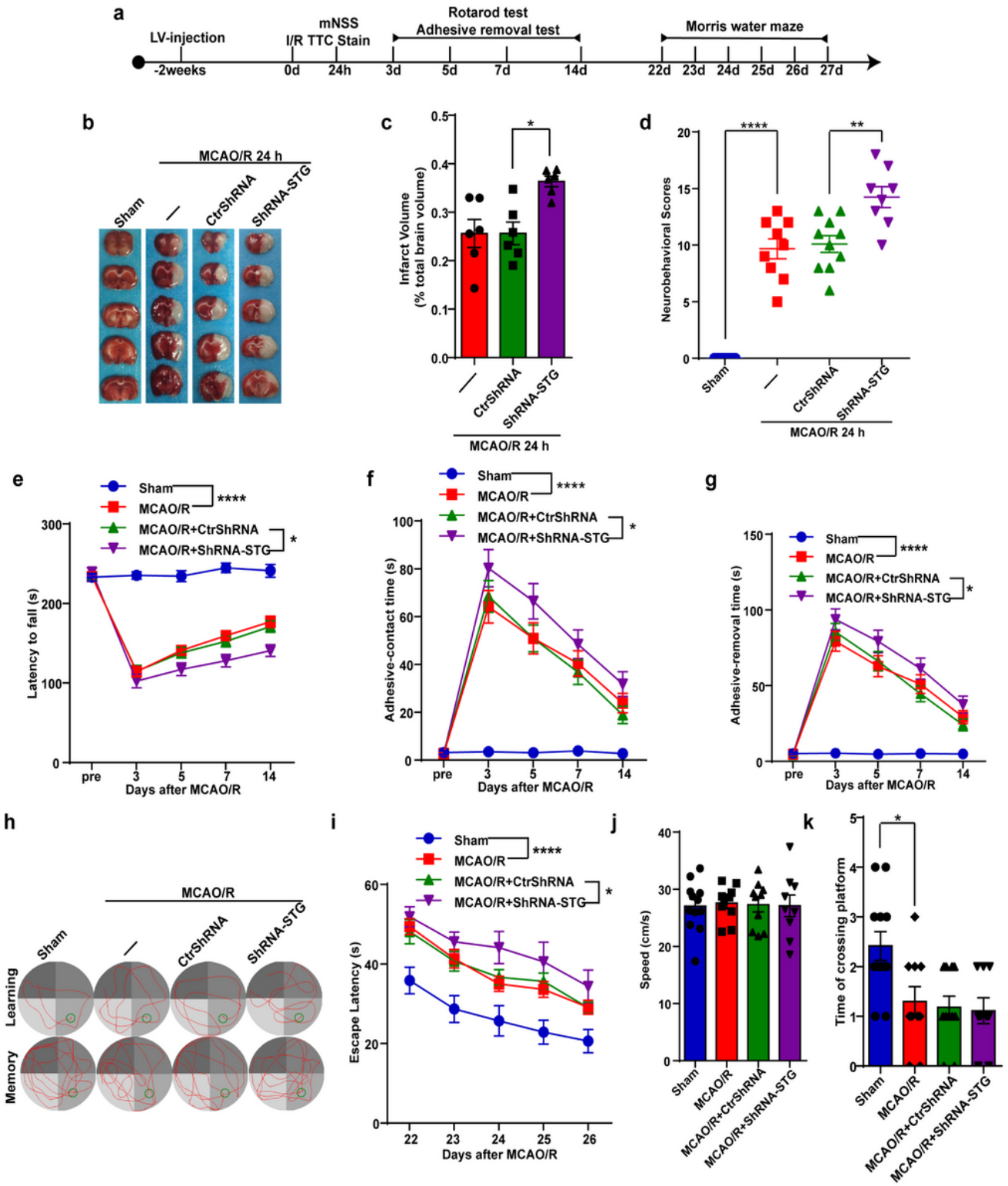

Figure 3

Effects of genetic knockdown of stargazin (STG) on brain injury. a. Timelines of the experimental procedure. b–c. Triphenyl tetrazolium chloride (TTC) staining of brain sections of MCAO/R rats after stargazin knockdown (MCAO/R 24 h + ShRNA-STG vs. MCAO/R 24 h + CtrShRNA, *P < 0.05, n = 6 per group). d. The Modified Neurological Severity Score (mNSS) test in MCAO/R rats after stargazin knockdown (MCAO/R 24 h vs. sham, ****P < 0.0001; MCAO/R 24 h + ShRNA-STG vs. MCAO/R 24 h +

CtrShRNA, **P < 0.01; n = 6 per group). e. Rotarod test (MCAO/R vs. sham, ****P < 0.0001; MCAO/R + ShRNA-STG vs. MCAO/R + CtrShRNA, *P < 0.05, n = 12 per group). f–g. Time to feel the adhesive tapes in the adhesive removal test (MCAO/R vs. sham, ****P < 0.0001; MCAO/R + ShRNA-STG vs. MCAO/R + CtrShRNA, *P < 0.05; n = 12 per group). h. Representative images illustrate the swim paths at 26 d (learning) and 27 d (memory) in the Morris water maze test after MCAO/R. i. Escape latency in the Morris water maze test at 22 to 26 d after MCAO/R (MCAO/R vs. sham, ****P < 0.0001, MCAO/R + ShRNA-STG vs. MCAO/R + CtrShRNA, *P < 0.05, n =12 per group). j. Swimming speed in the Morris water maze test at 27 d after MCAO/R. k. Times crossing the platform in the Morris water maze test at 27 d after MCAO/R (MCAO/R vs. sham, *P < 0.05, n = 12 per group). All data are presented as the mean ± SEM.

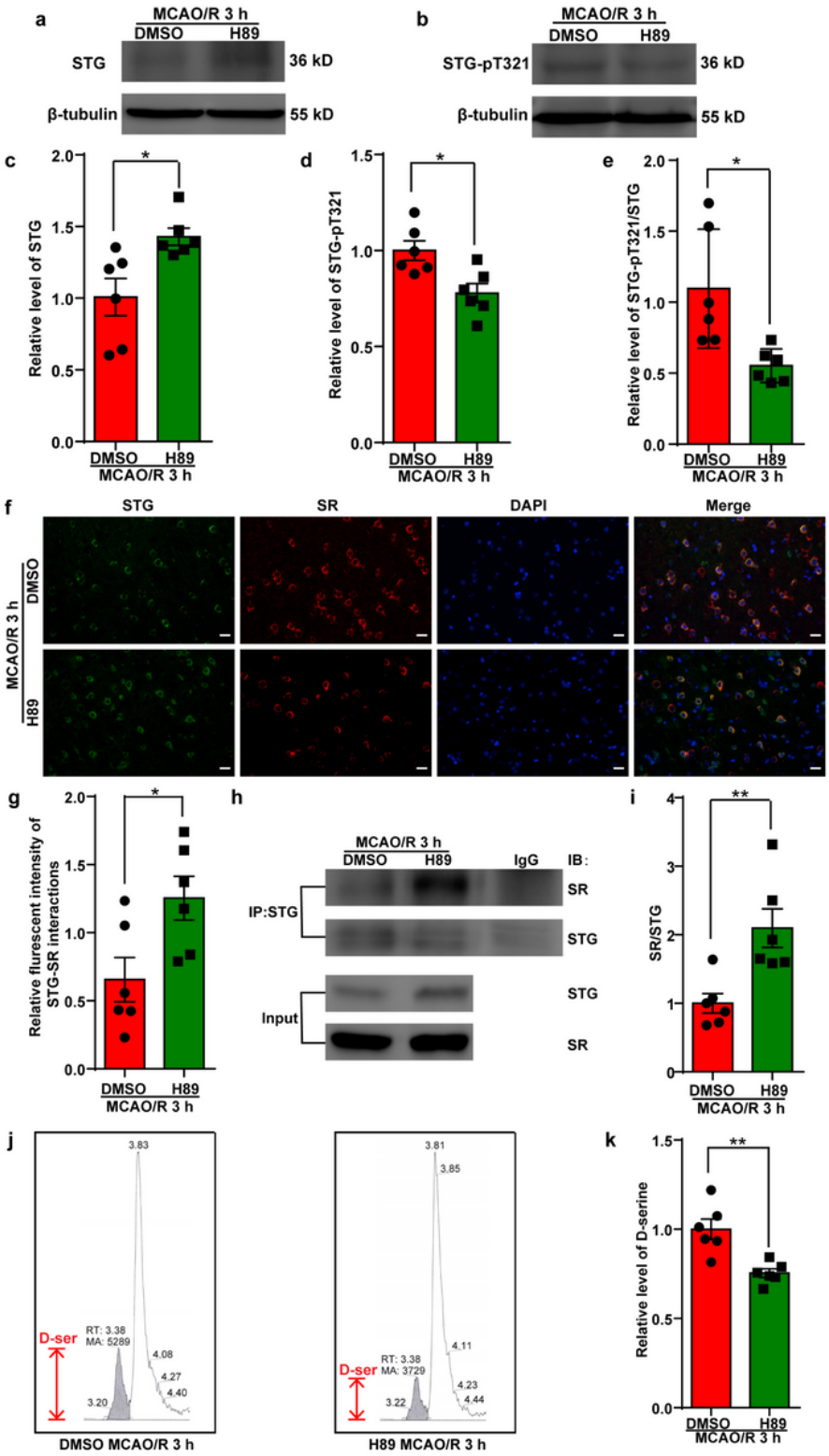

Figure 4

Effects of H89 on the phosphorylation level of stargazin-Thr-321 (STG-pT321), stargazin (STG) - serine racemase (SR) interaction and D-serine (D-ser) level. a–e. Western blot analysis of phosphorylation level of stargazin-Thr-321 in the ischemic penumbra of MCAO/R + DMSO/H89 rats (*P < 0.05 vs. MCAO/R + DMSO, n = 6 per group). f. Double immunofluorescence analysis was performed with antibodies against stargazin (green) and SR (red) in brain sections. Nuclei were fluorescently labeled with DAPI (blue).

Merged images show decreased colocalization of stargazin and SR at 3 hours (h) after MCAO/R + DMSO/H89. Scale bar: 20 μm. g. The relative fluorescent intensity of stargazin-SR interaction in penumbra tissue (*P < 0.05 vs. MCAO/R + DMSO, n = 6 per group). h–i. Coimmunoprecipitation and quantification of the interaction level of stargazin and SR in the ischemic penumbra of MCAO/R rats after DMSO/H89 injection (** P < 0.01 vs. MCAO/R + DMSO, n = 6 per group). j–k. Gas/liquid chromatography analysis and quantification of D-serine in the ischemic penumbra of MCAO/R rats after DMSO/H89 injection (**P < 0.01 vs. MCAO/R + DMSO, n = 6 per group). All data are presented as the mean ± SEM.

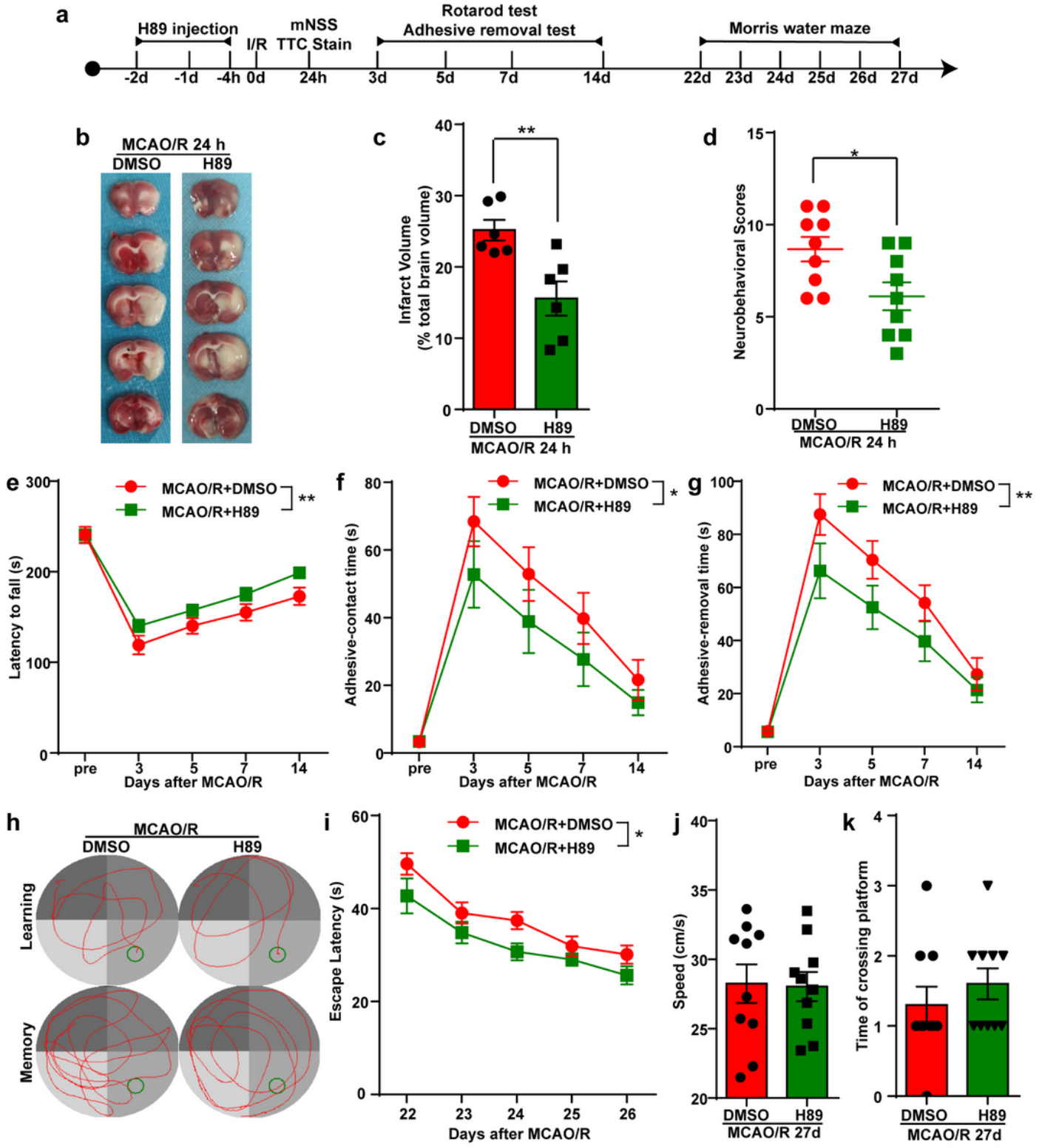

Figure 5

Effects of H89 on brain injury. a. Timelines of the experimental procedure. b–c. Triphenyl tetrazolium chloride (TTC) staining of brain sections at 24 hours (h) after MCAO/R + DMSO/H89 (**P < 0.01 vs. MCAO/R + DMSO, n = 6 per group). d. The Modified Neurological Severity Score (mNSS) test at 24 h after MCAO/R+ DMSO/H89 (*P < 0.05 vs. MCAO/R + DMSO, n = 6 per group). e. Rotarod test. (**P < 0.01 vs. MCAO/R + DMSO, n = 12 per group). f–g. Time to feel the adhesive tapes in the adhesive removal test (*P < 0.05 vs. MCAO/R + DMSO, **P < 0.01 vs. MCAO/R + DMSO, n = 12 per group). h. Representative images illustrate the swim paths at 26 day□d) (learning) and 27 d (memory) in the Morris water maze test after MCAO/R + DMSO/H89. i. Escape latency in the Morris water maze test at 22 to 26 d after MCAO/R+ DMSO/H89 (*P < 0.05 vs. MCAO/R + DMSO, n = 12 per group). j. Swimming speed in the Morris water maze test at 27 d after MCAO/R+ DMSO/H89 (n = 12 per group). k. Times crossing the platform in the Morris water maze test at 27 d after MCAO/R + DMSO/H89 (n = 12 per group). All data are presented as the mean ± SEM.

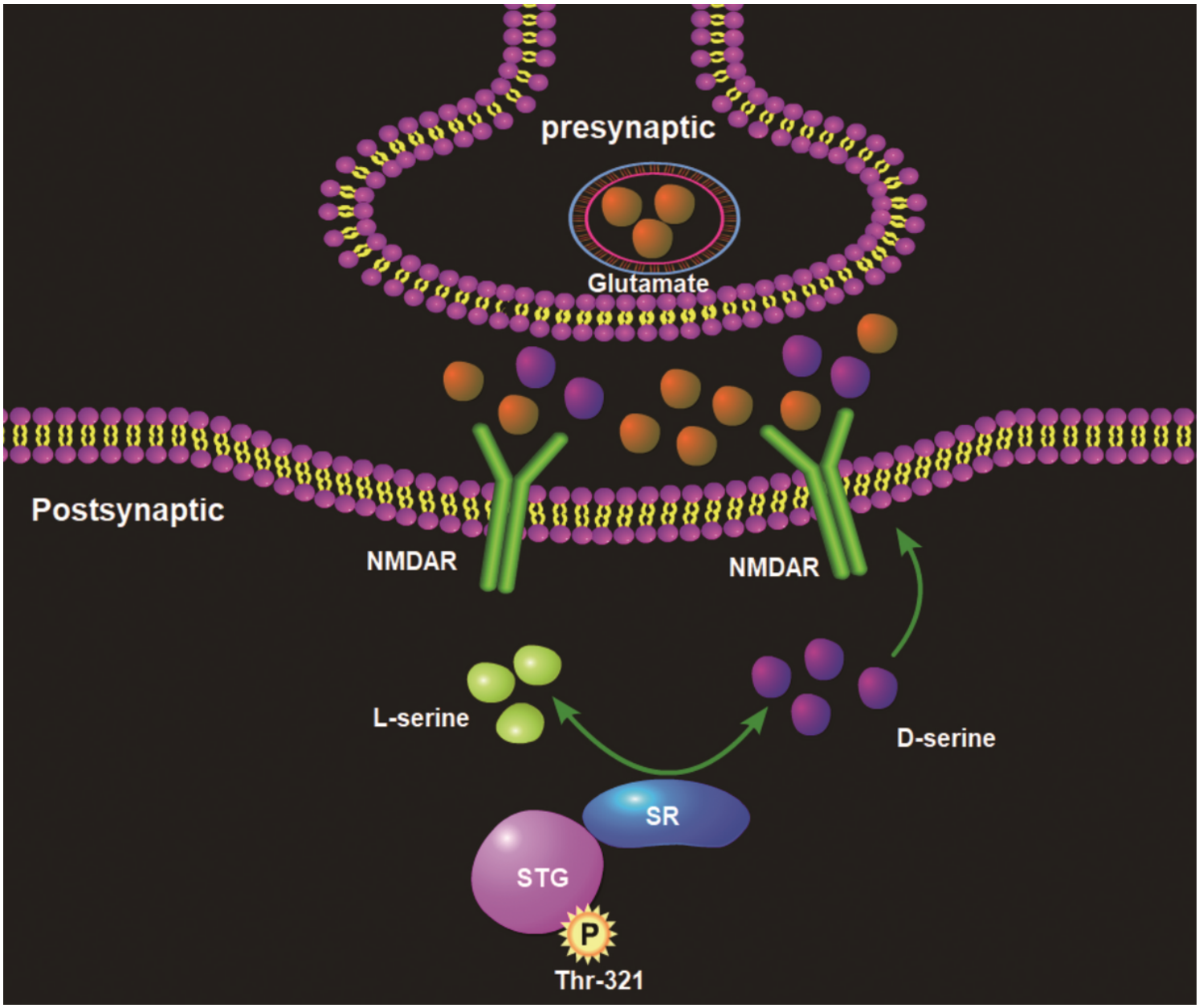

Figure 6

Schematic representations of potential mechanisms of stargazin interaction with serine racemase mediated cerebral ischemia/reperfusion injury in the MCAO/R model